

Electrical Detection of Spin Accumulation at a Ferromagnet-Semiconductor Interface

X. Lou,¹ C. Adelman,^{2,*} M. Furis,³ S. A. Crooker,³ C. J. Palmström,² and P. A. Crowell^{1,†}

¹*School of Physics and Astronomy, University of Minnesota, Minneapolis, Minnesota 55455, USA*

²*Department of Chemical Engineering and Materials Science, University of Minnesota, Minneapolis, Minnesota 55455, USA*

³*National High Magnetic Field Laboratory, Los Alamos National Laboratory, Los Alamos, New Mexico 87545, USA*

(Received 23 January 2006; published 3 May 2006)

We show that the accumulation of spin-polarized electrons at a forward-biased Schottky tunnel barrier between Fe and n -GaAs can be detected electrically. The spin accumulation leads to an additional voltage drop across the barrier that is suppressed by a small transverse magnetic field, which depolarizes the spins in the semiconductor. The dependence of the electrical accumulation signal on magnetic field, bias current, and temperature is in good agreement with the predictions of a drift-diffusion model for spin-polarized transport.

DOI: [10.1103/PhysRevLett.96.176603](https://doi.org/10.1103/PhysRevLett.96.176603)

PACS numbers: 72.25.Dc, 72.25.Mk, 85.75.-d

The injection and detection of spin-polarized electrons in semiconductors are two of the important problems in the physics of spin transport. Recent experiments have demonstrated that it is possible to maintain a nonequilibrium spin polarization greater than 25% in a semiconductor by injection of electrons from a ferromagnetic metal through a tunnel barrier [1–3]. In the case of a Schottky barrier, spin accumulation also occurs when electrons flow from the semiconductor to the ferromagnet [4–6]. In almost all cases, however, measuring the spin polarization in the semiconductor has required the use of optical techniques. This raises the important question of whether an electrically generated spin polarization at a ferromagnet-semiconductor interface can also be detected electrically. The strongest test of any electrical spin detection measurement is the existence of a Hanle effect [7,8], in which spin accumulation is suppressed by precession in a transverse magnetic field. A Hanle effect has not been observed in electrical measurements of spin accumulation in semiconductors reported previously [9–11]. In contrast, the *optical* Hanle effect has served as the basis for a series of definitive measurements of spin-dependent phenomena in semiconductors [12,13].

In this Letter, we report a direct electrical transport measurement of spin accumulation at an Fe/ n -GaAs interface in the presence of a forward-bias current. The existence of a spin accumulation is established using the electrical Hanle effect [7]. The spin-dependent voltage across the interface is suppressed by precession in a magnetic field applied perpendicular to the direction of spin polarization. The resulting peak in the voltage at zero magnetic field has a width determined by the time scales for spin precession, relaxation, drift, and diffusion. There is no corresponding electrical signature of spin injection under reverse bias, in agreement with a density of states argument based on tunneling.

The samples are grown on semi-insulating GaAs (100) substrates. We first grow a 300 nm undoped GaAs buffer

layer, followed by 2500 nm of Si-doped n -GaAs ($n = 3.6 \times 10^{16} \text{ cm}^{-3}$), which forms the channel of the device. The junction region consists of a 15 nm $n \rightarrow n^+$ -GaAs transition layer followed by 15 nm n^+ ($5 \times 10^{18} \text{ cm}^{-3}$) GaAs [1]. The Fe film, 5 nm thick, is then deposited epitaxially at $\sim 0^\circ \text{ C}$, followed by a 2 nm Al capping layer. A Schottky tunnel barrier is formed by the Fe and the n^+ -GaAs layer. The heterostructures are processed into Hall bars in which the n^+ -GaAs layer is removed everywhere except underneath the Fe contacts [see Fig. 1(a), in which the six Fe contacts are labeled $a-e$]. The source and drain contacts a and b are separated by $150 \mu\text{m}$, which is much longer than the spin diffusion length ($\sim 10 \mu\text{m}$ at 10 K) and spin drift length ($\sim 30 \mu\text{m}$ at 10 K and 1.0 mA). The easy magnetization axis of each $40 \times 100 \mu\text{m}$ Fe contact is parallel to the channel, which is along the GaAs [011] direction.

The calculated band diagram of the Fe/GaAs Schottky contacts is shown in Fig. 1(b) for three bias voltages covering the range of our experiment. Experimental I - V curves at $T = 10 \text{ K}$ are shown in the inset. In addition to the voltage V_{ab} measured from the source (reverse-biased) to the drain (forward-biased), we also measure the other voltages indicated in Fig. 1(a). This approach allows us to determine the voltage drops at the source and drain contacts independently.

The lateral geometry allows us to use the approach of Ref. [6] to image the electron spin polarization, which we observe at both the source and drain electrodes in the presence of a current. The polarization near the source electrode is due to spin injection through the Schottky barrier [1,3,14], while the spin accumulation at the drain electrode is due to the spin-dependent reflectivity of the barrier under forward bias [4,5,15]. In either case, the polarization in the semiconductor is oriented antiparallel to the magnetization of the Fe contact [6] and is suppressed by applying a magnetic field of $\sim 100 \text{ Oe}$ perpendicular to the magnetization axis, demonstrating the existence of a Hanle effect.

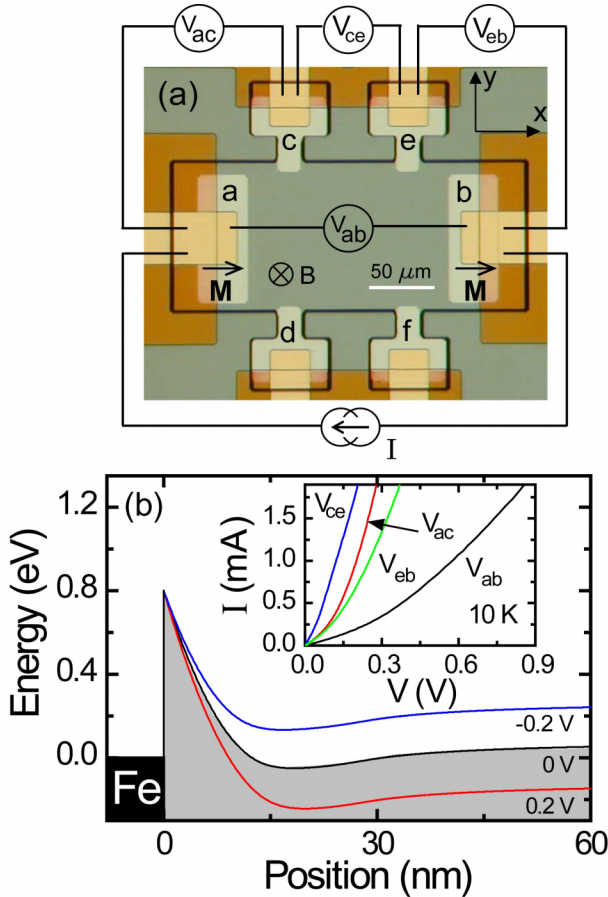


FIG. 1 (color online). (a) Photomicrograph of the Fe/GaAs device. The side contacts are used for the voltage measurements indicated by the labels. (b) Band diagram near the Fe/GaAs interface under reverse bias (0.2 V), zero bias (0 V), and forward bias (-0.2 V). The inset shows the total (V_{ab}), drain (V_{ac}), source (V_{eb}), and channel (V_{ce}) voltage measurements when current flows from a to b at $T = 10$ K.

Given the existence of nonequilibrium spin populations at the source and the drain, we consider the electrical transport properties of the device when a small magnetic field ($H \ll 4\pi M$) is applied perpendicular to the plane of the structure. In this geometry, the magnetization of each electrode remains fixed. Figure 2(a) shows voltage measurements (with an offset subtracted from each curve) at 10 K for a 0.8 mA bias current flowing from contact a to b , so that electrons are flowing from b (source) to a (drain). The total source-drain voltage drop V_{ab} is approximately 0.5 V. The important feature of Fig. 2(a) is the peak at zero field in the total voltage V_{ab} as well as the drain voltage V_{ac} . These two measurements nearly coincide and have an amplitude $\Delta V \sim 60 \mu\text{V}$ and full-width at half maximum (FWHM) ~ 40 Oe. In contrast, no peak is observed in the source and channel voltages V_{eb} and V_{ce} . When the current direction in the channel is reversed [Fig. 2(b)], the peak is observed only for the voltage measurements that include contact b , which is now the drain. The amplitude and FWHM of the peak are the same as in Fig. 2(a).

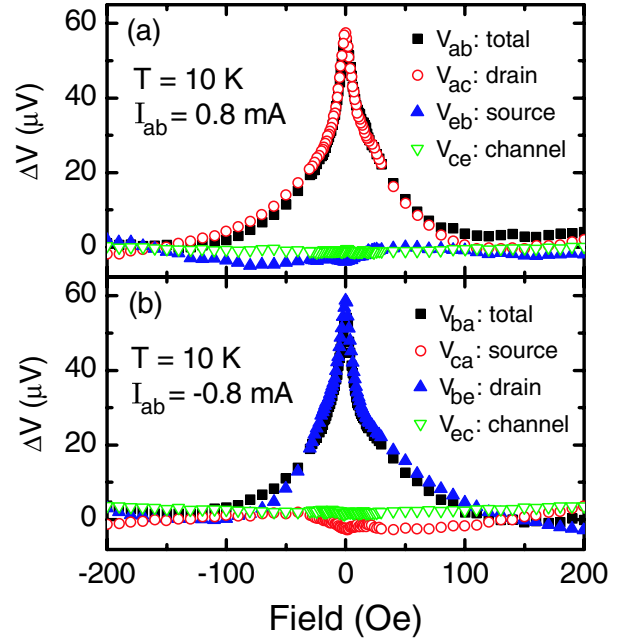


FIG. 2 (color online). (a) Voltage vs magnetic field for a current $I = 0.8$ mA flowing from a to b . The source-drain voltage $V_{ab} \approx 0.5$ V. An offset is subtracted from each curve, and a slope due to the Hall effect has been subtracted from V_{ac} and V_{eb} . The contacts are labeled in Fig. 1(a). (b) Measurements for $I = 0.8$ mA flowing from b to a . The peak at zero field appears only for measurements that include the drain contact.

The asymmetry between source and drain shown in Fig. 2 has been observed in every Fe/GaAs device of this design over the channel doping range from 2×10^{16} to $1.5 \times 10^{17} \text{ cm}^{-3}$. No peak is observed in devices in which the Fe has been replaced by Al. Since the electrode magnetization remains fixed, stray magnetic fields or anisotropic magnetoresistance can be excluded as possible origins of the effect.

The voltage peak at zero field observed at the drain contact is a signature of spin accumulation at the ferromagnet-semiconductor interface. The effective resistance of the Schottky barrier is higher when a spin accumulation in the semiconductor is present. This is consistent with the model of Ciuti *et al.* [15], in which the barrier is less transmissive for the spin state that accumulates in the semiconductor. The accumulation is suppressed by precession of the spin in a transverse field, leading to a decrease in the voltage. This explanation is also consistent with information inferred from the optical detection experiments [6], with which a more detailed comparison will be made below. As noted above, however, a nonequilibrium spin polarization is detected optically at *both* the source and drain electrodes, but the zero-field peak in the voltage is observed only at the drain contact. This reflects the fact that the Fe/GaAs interface acts as a tunnel barrier. At the reverse-biased source contact, the injected electrons tunnel from filled states in Fe into empty states in GaAs. These states are at an energy $eV_s \gg k_B T$ above the quasi-

Fermi level for each spin, where V_s is the voltage drop across the source contact. The fractional occupancy of these states is therefore small, and so the number of available states for each spin is essentially the same. As a result, the tunneling resistance under reverse bias does not depend on the spin polarization in the semiconductor. Under forward bias, both the filled states in the GaAs and the empty states in Fe are polarized. In this case, the tunneling current should be sensitive to the spin polarization in the semiconductor, as is observed experimentally.

Measurements of ΔV_{ab} for different temperatures at a fixed bias current of 1.0 mA are shown in Fig. 3(a). To model these data, we adopt an approach used previously for spin-dependent transport in metals [7,8], but in this case the spins are generated and detected at a single ferromagnetic contact (the drain). The electrons in GaAs are polarized with an orientation along the magnetization axis \hat{x} by scattering from the interface at x_1 [15]. This process creates spin polarization at a rate S_0 per unit contact length. The spins then drift and diffuse under the contact before being detected at some time t at x_2 . The spins also precess about the applied field B and decay with a relaxation time τ_s . The x component of the steady-state spin polarization $S_x(x_1, x_2, B)$ at x_2 due to spin generated at x_1 is obtained by

integrating the Green's function solution of the drift-diffusion equation (including the spin relaxation and precession terms) over time, so that [5–8]

$$S_x(x_1, x_2, B) = \int_0^\infty \frac{S_0}{\sqrt{4\pi Dt}} e^{-(x_2-x_1+v_d t)^2/4Dt-t/\tau_s} \times \cos\left(\frac{g\mu_B B}{\hbar} t\right) dt, \quad (1)$$

where D is the diffusion constant, v_d is the drift velocity, $g = -0.44$ is the g factor for electrons in GaAs, and μ_B is the Bohr magneton. The average spin polarization $S_x(B)$ is determined by integrating $S_x(x_1, x_2, B)$ over x_1 and x_2 , which vary from 0 to L , where $L = 40 \mu\text{m}$ is the length of the drain contact.

With the exception of S_0 , the parameters in Eq. (1) are determined at each temperature by independent measurements. v_d is calculated from the current using the carrier density determined from Hall measurements, and D is determined from the measured Hall mobility [16]. The lifetime τ_s is determined by the optical Hanle effect as measured by Kerr rotation. We assume that the voltage drop at the drain is proportional to $S_x(B)$ and fit the data in Fig. 3(a) with S_0 (effectively the amplitude of the peak) as the only free parameter.

This procedure produces good agreement with the data at high temperatures, but the widths of the modeled peaks at 10 K are too small by approximately a factor of 2. This reflects a greater sensitivity to the time L/v_d for the electrons to drift across the contact. In practice, the current through the interface will be concentrated near the upstream edge of the contact, with a distribution determined by the resistances of the channel and the interface, which are comparable [see inset in Fig. 1(b)]. We account for this by integrating over an effective length $L_e < L$ that is adjusted to fit one set of data (at 10 K) and then fixed for all other data sets. The solid curves in Fig. 3(a) are calculated using $L_e = 15 \mu\text{m}$.

An important aspect of the data that is predicted by the model is the increase in the FWHM of the peak as T increases above 30 K. This is due to the temperature dependence of τ_s [17], which decreases in this sample from 45 nsec at 10 K to 5 nsec at 60 K. The peaks continue to broaden and decrease in amplitude above 60 K, but they can no longer be resolved above 80 K.

The field dependence of the spin polarization that we measure electrically is the same as that found by more traditional optical methods. To demonstrate this, a small magnetic field is applied in the plane of the sample (perpendicular to the magnetization), and the spin polarization is measured using Kerr microscopy [6]. Electrically injected spins precess into the z direction, leading to a Kerr rotation θ_K proportional to S_z . Figure 3(b) shows θ_K measured at the edge of the source contact at three different temperatures. The solid curves are generated using the same parameters as for the transport data in Fig. 3(a) (except for the amplitude), with Eq. (1) modified to account for the fact

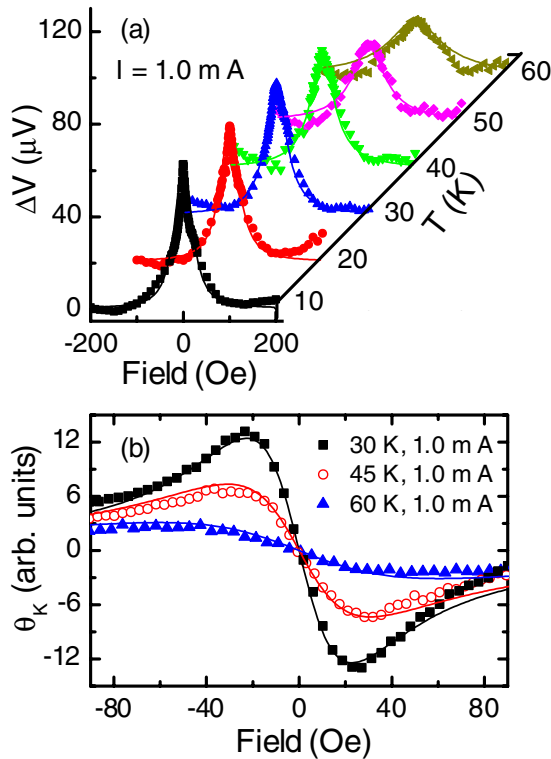


FIG. 3 (color online). (a) The source-drain voltage ΔV_{ab} is shown as a function of magnetic field and temperature. Solid lines are the results of the modeling explained in the text. (b) The Kerr rotation θ_K (proportional to S_z), measured near the source, is shown as a function of magnetic field for three temperatures. The solid curves are calculated using the same parameters used to fit the transport data.

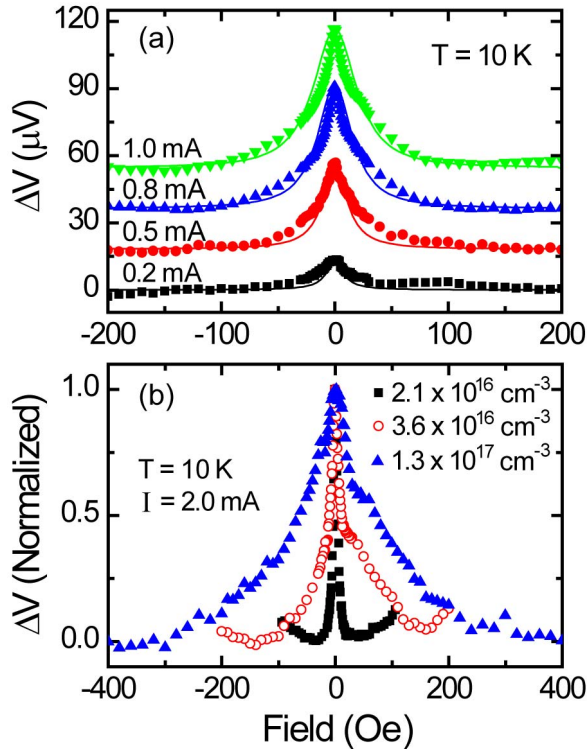


FIG. 4 (color online). (a) ΔV_{ab} vs magnetic field at $T = 10$ K for four different bias currents. Each curve is offset for clarity. The solid lines are the fitted curves using the model explained in the text. (b) ΔV_{ab} at $T = 10$ K and $I = 2.0$ mA for three different n -type samples.

that θ_K is sensitive to S_z rather than S_x . In this case, the integration extends only over the source coordinate. The agreement with experiment provides extremely strong support for the interpretation of the transport measurements.

Besides τ_s , the other time scales that can determine the FWHM of ΔV are L_e^2/D , L_e/v_d , and $4D/v_d^2$. These have little effect at high temperature because they are all much larger than τ_s . At low temperatures, however, the time scales that depend on v_d become shorter than τ_s at the highest currents. ΔV_{ab} is shown for several currents at 10 K in Fig. 4(a). The solid curves are generated from the model with $L_e = 15$ μm . The amplitude is nearly proportional to the current. The FWHM of the model curves also increases with current, due primarily to the fact that L_e/v_d decreases from 130 nsec at 0.2 mA to 20 nsec at 1.0 mA. The limiting width at small bias is set by spin relaxation ($\tau_s = 45$ nsec at 10 K) and diffusion.

The width also increases with bias current in the experimental data. At the highest currents, however, the peaks become sharper in the region $|B| < 10$ Oe. This can be seen more prominently in Fig. 4(b), which shows ΔV_{ab} at a current of 2.0 mA for this sample ($n = 3.6 \times 10^{16}$ cm^{-3}) and two others with different channel dopings. The narrow features near zero field become stronger with decreasing doping and are characteristic of an enhancement of the effective magnetic field acting on the electrons due to

dynamic polarization of nuclei [18]. This effect is regularly observed in optical pumping experiments and is also seen in optical measurements of the spin accumulation under forward bias [4,5]. Excluding very small fields, Fig. 4(b) shows an overall correlation between the FWHM and increasing doping that is expected given the dependence of τ_s on carrier density [17,19].

The measurements discussed here show that the electrically generated spin accumulation at a forward-biased Fe/ n -GaAs Schottky contact can also be detected electrically. A quantitative comparison is made with the established approach of optical detection. The results demonstrate that it is possible to determine important parameters of a semiconductor spin transport device using electrical measurements alone.

This work was supported by the DARPA SpinS and Los Alamos LDRD programs, the NSF MRSEC program under DMR 02-12032, ONR, and the NSF NNIN program through the Minnesota Nanofabrication Center.

*Present address: IMEC, 3000 Leuven, Belgium.

†Electronic address: crowell@physics.umn.edu

- [1] A. T. Hanbicki *et al.*, Appl. Phys. Lett. **82**, 4092 (2003).
- [2] X. Jiang *et al.*, Phys. Rev. Lett. **94**, 056601 (2005).
- [3] C. Adelmann *et al.*, Phys. Rev. B **71**, 121301(R) (2005).
- [4] R. J. Epstein *et al.*, Phys. Rev. B **68**, 041305(R) (2003); R. K. Kawakami *et al.*, Science **294**, 131 (2001); R. J. Epstein *et al.*, Phys. Rev. B **65**, 121202(R) (2002).
- [5] J. Stephens *et al.*, Phys. Rev. Lett. **93**, 097602 (2004).
- [6] S. A. Crooker *et al.*, Science **309**, 2191 (2005).
- [7] M. Johnson and R. H. Silsbee, Phys. Rev. Lett. **55**, 1790 (1985); Phys. Rev. B **37**, 5326 (1988).
- [8] F. J. Jedema *et al.*, Nature (London) **416**, 713 (2002).
- [9] P. R. Hammar, B. R. Bennett, M. J. Yang, and M. Johnson, Phys. Rev. Lett. **83**, 203 (1999); P. R. Hammar and M. Johnson, Phys. Rev. Lett. **88**, 066806 (2002).
- [10] R. Mattana *et al.*, Phys. Rev. Lett. **90**, 166601 (2003).
- [11] G. Schmidt *et al.*, Phys. Rev. Lett. **87**, 227203 (2001).
- [12] *Optical Orientation*, edited by F. Meier and B. P. Zakharchenya (North-Holland, Amsterdam, 1984).
- [13] A recent example is the demonstration of the spin Hall effect: Y. K. Kato, R. C. Myers, A. C. Gossard, and D. D. Awschalom, Science **306**, 1910 (2004).
- [14] H. J. Zhu *et al.*, Phys. Rev. Lett. **87**, 016601 (2001).
- [15] C. Ciuti, J. P. McGuire, and L. J. Sham, Phys. Rev. Lett. **89**, 156601 (2002); J. P. McGuire, C. Ciuti, and L. J. Sham, Phys. Rev. B **69**, 115339 (2004); for other approaches, see V. V. Osipov and A. M. Bratkovsky, Phys. Rev. B **72**, 115322 (2005); G. E. W. Bauer *et al.*, Phys. Rev. B **72**, 155304 (2005).
- [16] M. E. Flatté and J. M. Byers, Phys. Rev. Lett. **84**, 4220 (2000).
- [17] J. M. Kikkawa and D. D. Awschalom, Phys. Rev. Lett. **80**, 4313 (1998).
- [18] V. G. Fleisher and I. A. Merkulov, in Ref. [12]. The dynamic polarization is due to a small ($\sim 1^\circ$) misalignment of our sample.
- [19] R. I. Dzhioev *et al.*, Phys. Rev. B **66**, 245204 (2002).